Geometrical models of interface evolution. III. Theory of dendritic growth

David A. Kessler
Department of Physics, Rutgers University, Piscataway, New Jersey 08854

Joel Koplik and Herbert Levine
Schlumberger-Doll Research, Old Quarry Road, Ridgefield, Connecticut 06877-4108

(Received 26 June 1984)

We construct a theory of velocity selection and tip stability for dendritic growth in the local evolution model. We show that the growth rate of dendritic patterns is determined by a nonlinear solvability condition for a translating finger. The sidebranching instability is related to a single discrete oscillatory mode about the selected velocity solution, and the existence of a critical anisotropy is shown to be due to the zero crossing of its growth rate. The marginal-stability hypothesis cannot predict the correct dynamics of this model system. We give heuristic arguments that the same ideas will apply to dendritic growth in the full diffusion system.

I. INTRODUCTION

In a previous series of papers[1,2] (hereafter referred to as I and II) we have constructed a local geometrical evolution model for the process of dendritic crystal growth. This model assumes that the interface $\mathbf{x}(s)$ between the growing solid and the supercooled melt satisfies the equation

$$\hat{\mathbf{n}}\cdot\frac{d\mathbf{x}}{dt}=\left[\kappa+A\kappa^2-B\kappa^3+\frac{d^2\kappa}{ds^2}\right][1+\epsilon\cos(m\theta)]\,, \qquad (1)$$

where $\hat{\mathbf{n}}$ is the curve normal making an angle θ with the $\hat{y}$ axis, s is the arclength, $\kappa=d\theta/ds$ is the curvature, and A and B are parameters representing the undercooling and minimum bubble size, respectively. The term proportional to ϵ is due to crystal anisotropy, reflecting enhanced growth along the m-fold symmetry axes. In this paper we will restrict ourselves to $m=4$, but we have seen in II that the results do not change qualitatively with m. For a detailed discussion of (1), see Refs. 1 and 2.

Let us briefly review the phenomenology of Eq. (1) as it relates to dendritic growth. By a dendrite[3] we mean a moving tip which exhibits oscillatory behavior connected to the emission of sidebranches, which in turn behave as new dendritic tips. A typical example of this type of growth is depicted in Fig. 1. In II we demonstrated that this model gives rise to stable dendritic growth if and only if the anisotropy ϵ is greater than a critical anisotropy ϵ_c depending on A, B, and m, but not on the initial conditions. We discussed how the "marginal-stability hypothesis" of Langer and Müller-Krumbhaar[4] was in contradiction with our results and concluded that further theoretical understanding of dendritic growth was required.

The purpose of this paper is to present a new and comprehensive approach to the velocity selection and tip-stability problems in this type of system. We will show that the continuous family of steady-state solutions with arbitrary velocity present in the absence of surface tension breaks down to a discrete set of solutions, each with a unique velocity. (A similar behavior was discovered in a related context by McLean and Saffman, and Vanden-Broeck.[5] This will be discussed later.) The largest of these velocities is most likely to give rise to stable growth (because it can, so to speak, outrun instabilities) and it therefore is dynamically "selected." Whether or not this solution is indeed stable is then answered by a study of the eigenvalue spectrum of the linear-stability operator. As ϵ crosses from below $\epsilon_c(A,B,m)$ to above, the real part of the leading discrete complex eigenvalue becomes negative, signifying tip stability in the moving frame of reference.

The major question raised by our work is how applicable our results are to more realistic solidification models incorporating global diffusion-driven dynamics. We believe that there is an excellent chance that our selection mechanism *directly* carries over to these other systems, so

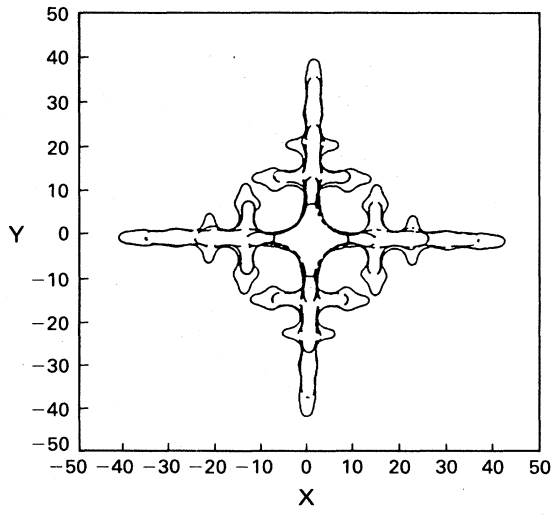

FIG. 1. Example of dendritic growth in the local evolution model ($A=4.0$, $B=1.5$, $\epsilon=0.15$).

that the marginal-stability hypothesis would not apply to these cases. It would remain valid for the description of certain one space-dimensional partial differential equations,[6] and perhaps in other contexts as well. In the last section of this paper we present our reasons for believing this to be the case. We are currently attacking this problem by a combination of numerical and analytical methods and hope to report on this subject in the near future.

II. STEADY-STATE SOLUTIONS

In I we discussed how our local model, in the absence of the $d^2\kappa/ds^2$ "surface-tension" term, exhibited a continuous family of steady-state dendritic solutions corresponding to arbitrary tip velocities. To see this, note that $\hat{n}\cdot d\mathbf{x}=V\cos\theta$ for any uniformly translating solution. Equation (1) then reduces to a third-order algebraic equation for $\kappa=d\theta/ds$. We can integrate this equation from $s=0$, $\theta=0$; $\kappa(0)$ is determined algebraically and $\kappa'(0)$ equals zero automatically. For large arclength, the solution approaches

$$\frac{V\cos\theta}{1+\epsilon}=\kappa \tag{2}$$

which integrates to the asymptotic shape

$$y=\rho\ln\cos(x/\rho)\ , \tag{3}$$

where $\rho=(1+\epsilon)/V$. The dendrite approaches the fixed point $\theta=\pi/2$ exponentially, regardless of the value of the velocity. This family of solutions is the model's analog of the Ivantsov needle crystal.[7]

When we include the surface-tension term $d^2\kappa/ds^2$, we argued in I that, in general, there would be no steady-state solution at arbitrary V. This comes about because of an incompatibility of the condition $\kappa'(0)=0$ with the required approach to the $\theta=\pi/2$ fixed point. Defining $\beta=d\kappa/ds$, the evolution equation can be written as the autonomous system

$$\frac{d\kappa}{ds}=\beta\ ,\quad \frac{d\theta}{ds}=\kappa\ ,$$

$$\frac{d\beta}{ds}=\frac{V\cos\theta}{1+\epsilon\cos(m\theta)}-\kappa-A\kappa^2+B\kappa^3\ .$$

There is a fixed point at $\theta=\pi/2$, $\kappa=\beta=0$, which the solution should approach for large s. Linearizing about this fixed point and assuming that the variables behave as $e^{-\alpha s}$, we find the eigenvalue equation $V/(1+\epsilon)=\alpha+\alpha^3$. One root is real and positive, corresponding to the exponential approach to the fixed point. To find the other roots, if we let $\alpha=\alpha_r+i\alpha_i$, then

$$0=\alpha_i+\alpha_i(3\alpha_r^2-\alpha_i^2)\ ,\quad \frac{V}{1+\epsilon}=-2\alpha_r(1+4\alpha_r^2)\ .$$

These roots are complex conjugate and, since $\alpha_r<0$, they correspond to eigenvectors which exponentially diverge going down the dendrite. Thus, the requirement that κ, θ, and β approach the fixed point determines a unique trajectory, all the way back to $\theta=0$, which we hereafter label as $s=0$. One therefore expects, in general, that $\beta(0)=\kappa'(0)\neq 0$ and so a well-behaved symmetric dendrite does not exist. In I we showed that for $A=B=\epsilon=0$ there were in fact no solutions of the steady-state equation.

To further investigate the issue of steady-state solutions, we picked initial conditions such that we sat exactly on the converging eigenvector in the near vicinity of the fixed point (i.e., $\kappa=10^{-10}$). We then integrated backward in s until θ equalled zero, and determined β. If β crosses zero as the velocity is varied, we can identify a *discrete* set of possible velocities for uniformly translating shapes. A typical plot of $\beta(V)$ is shown in Fig. 2. Notice that there is, in general, a discrete set of solutions culminating in a maximal velocity solution V^*. As we will discuss later, increasing V always corresponds to increased stability; V^* is thus the most stable (but not necessarily stable) steady-state dendrite.

In Fig. 3 we plot V^* as a function of A for fixed B and ϵ, ϵ for fixed A and B, and B for fixed A and ϵ. This graph is consistent with the idea that A represents the undercooling. The larger the undercooling, the larger V^*. In fact, for $B=\epsilon=0$, $V^*\to 0$ as $A\to 0$. This is consistent with the aforementioned absence of solutions in the special case considered in I.

The key fact we wish to state in this section is that V^* is *exactly* equal to the average tip velocity as given by our numerical simulations in II. We have checked this for a wide variety of cases involving variations of all parameters A, B, and ϵ. The velocity-selection mechanism in this system is thus simply the solvability condition for the steady-state equation. The maximal velocity is selected due to its being the most stable with respect to tip-splitting perturbations. We will see this in detail in Sec. III.

Our results are in direct contrast to those predicted by the marginal-stability hypothesis as it is usually applied to dendrite-forming systems. In this approach the system "chooses" a velocity such that the steady-state solution is

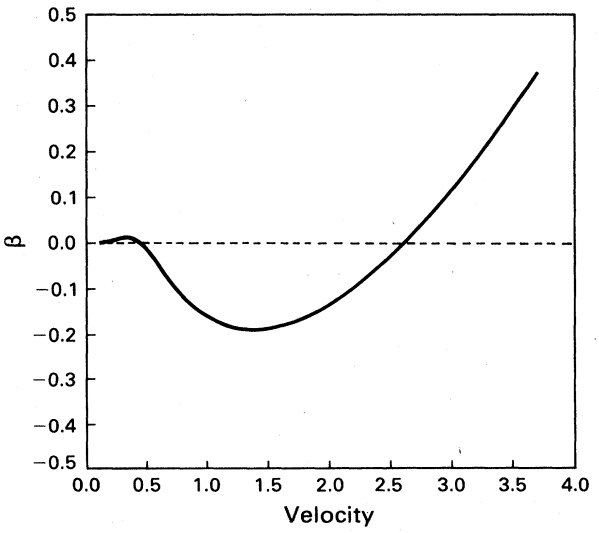

FIG. 2. $\beta(0)$ as a function of velocity for steady-state solutions.

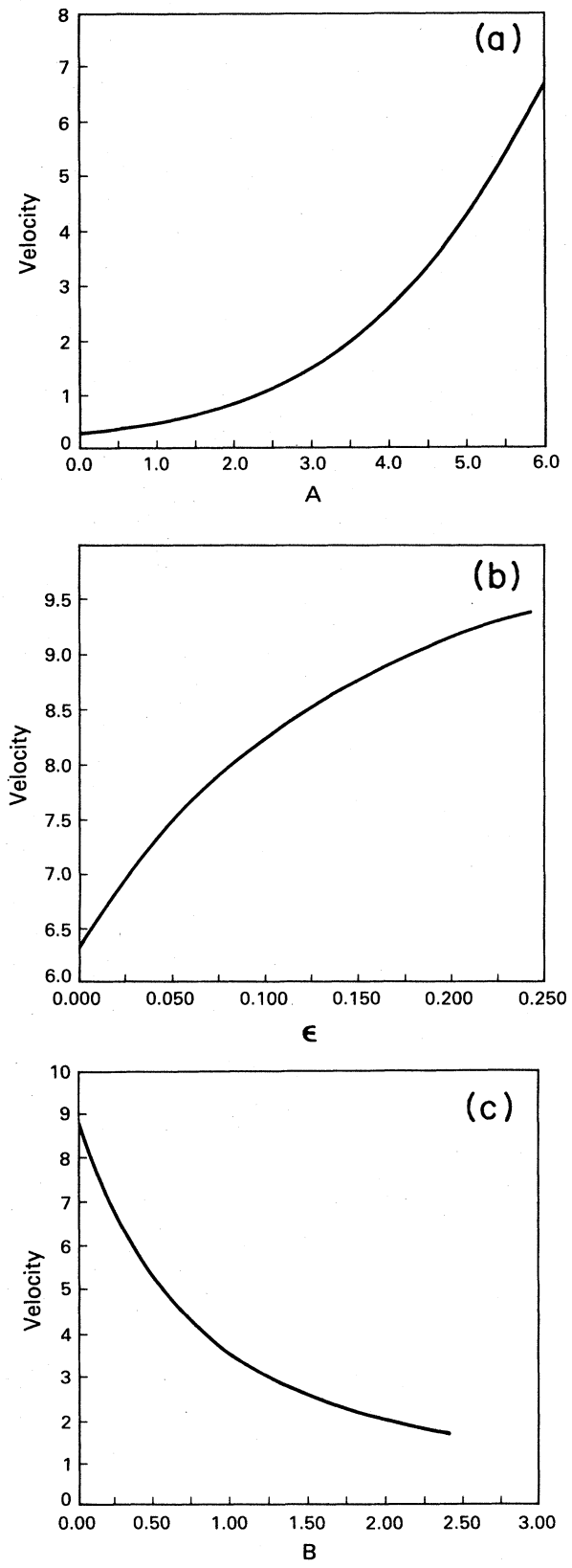

FIG. 3. Maximal velocity V^* as a function of (a) A at $B=1.5$ and $\epsilon=0.15$, (b) ϵ at fixed $A=4.0$ and $B=0.0$, and (c) B at fixed $A=4.0$ and $\epsilon=0.15$.

marginally stable to small perturbations. In our theory stability is only of concern once the velocity has been determined by a nonlinear eigenvalue constraint. Our system can and does operate away from the marginally stable point. Our analysis does, however, bear some resemblance to the ideas which underlie the work of Aronson and Weinberger.[6] In particular, we use a discrete "maximum-velocity" principle, whereas previous work used a continuous version of that idea. We will later present evidence that our version stands a better chance of carrying over to more complete solutions of the dendrite problem.

III. STABILITY ANALYSIS

In II we showed that dendritic growth would be stable only for $\epsilon > \epsilon_c$. In particular, we plotted the tip velocity as a function of time and followed the change from growing to decaying oscillations as the anisotropy was increased. We now show that our solvability mechanism for velocity selection can also explain these results.

Let us assume that the curve $\mathbf{x}(s)$ is given by a small perturbation around the steady-state solution $\mathbf{x}=\mathbf{x}_0+\hat{\mathbf{n}}\delta(s)$. It is easy to see that to linear order, $\theta=\theta_0-\delta'$, $\kappa=\kappa_0-\delta''-\kappa_0^2\delta$ (where the prime means d/ds_0). Substituting these expressions into (1), we derive the linear-stability equation

$$\frac{\dot{\delta}}{1+\epsilon\cos(m\theta)}=-\delta''''+C_2\delta''+C_1\delta'+C_0\delta\ , \tag{4a}$$

where

$$\begin{aligned} C_0&=-\kappa_0^2U'(\kappa_0)-4\kappa_0\kappa_0''-3(\kappa_0')^2\ ,\\ C_1&=-5\kappa_0\kappa_0'+V[U'(\kappa_0)+\kappa_0''']/\kappa_0\ ,\\ C_2&=-U'(\kappa_0)-\kappa_0^2\ , \end{aligned} \tag{4b}$$

with $U(\kappa)\equiv\kappa+A\kappa^2-B\kappa^3$. We now look for solutions of the form $\delta_k(t)\sim e^{\omega_k t}\delta_k(s)$. Stable dendrites require $\mathrm{Re}\omega_k<0$ for all eigenvalues k.

Fourth-order stability equations are a common feature of boundary-layer problems in fluid mechanics, and our approach to this equation will be modeled on the work of Mack[8] on the Orr-Sommerfeld equation. In such situations there can occur both discrete and continuous eigenvalue spectra, corresponding to different ways in which the eigenfunctions δ can satisfy the boundary conditions imposed on the perturbation. We will see shortly how this works in our case.

Let us consider the asymptotic (i.e., large s) form of Eq. (4), which can be written in the form

$$\frac{\omega\delta}{1+\epsilon}=-\delta''''-\delta''-\frac{V\sin\theta}{1+\epsilon}\delta'\ , \tag{5}$$

where $\sin\theta=\pm1$ depending on which side of the tip we are on. Assuming $\delta\sim e^{qs}$, we find the asymptotic dispersion relation

$$\frac{\omega}{1+\epsilon}=-q^4-q^2+\frac{Vq}{1+\epsilon}\ .$$

We label the four roots in decreasing order of their real parts and try to form a solution which satisfies two (arbitrary) boundary conditions at $s=-L$ $(\rightarrow-\infty)$. To do

this we must pick coefficients in the expansion

$$\delta=\sum_{i=1}^{4}\delta_i e^{q_i s}$$

to ensure three terms of the same approximate magnitude at $s=-L$. This requires $\delta_4\sim e^{-(q_2-q_4)L}\delta_2$ and $\delta_3\sim e^{-(q_2-q_3)L}\delta_2$, where $\mathrm{Re}(q_2-q_4)\geq\mathrm{Re}(q_2-q_3)\geq 0$.

Now, these solutions can be extended to the region around $s=0$ where $e^{q_i s}$ is replaced by an $O(L^0)$ function $\phi_i(s)$, and we must impose $\delta'(0)=\delta'''(0)=0$. In general, we only have two coefficients δ_1 and δ_2 at our disposal and this cannot be done. The only possibilities for satisfying the boundary conditions are $\mathrm{Re}q_2=\mathrm{Re}q_3$, or an accidental degeneracy in the $s=0$ conditions. The first gives rise to a continuous spectrum and the second to a discrete set of eigenvalues.

The first possibility was investigated in I with the following result: the most unstable mode crossed below $\mathrm{Re}\omega=0$ at the point when $V^2(1+\epsilon)^2\cong 2.65$. This velocity is much lower than, say, the actual velocity selected at $A=4$, $B=+1.5$, $\epsilon=0.14$ (see Fig. 3) which in II was shown to be unstable. This suggests that discrete modes exist above the continuum. For this to occur a degeneracy is needed and the above argument yields the condition

$$\Psi(\omega)\equiv\det\begin{bmatrix}\phi_1'(0) & \phi_1'''(0)\\ \phi_2'(0) & \phi_2'''(0)\end{bmatrix}=0\ . \tag{6}$$

To find Ψ we must integrate the stability equation from large negative s and find the continuation of the solutions which behave asymptotically as $e^{q_{1,2}s}$. First we found the selected velocity to 10^{-6} accuracy and identified the coefficients C_0, C_1, C_2 by spline interpolation using values every 0.01 arclength units. Then we used a predictor-corrector ordinary differential equation (ODE) solver to integrate the two solutions ϕ_1 and ϕ_2 forward from $s=10^{-10}$ towards $s=0$. In addition, after every $\Delta s=3$ step we orthogonalized ϕ_2 with respect to ϕ_1 in order to reduce the error due to an admixture of an exponentially growing ϕ_1 piece in the ϕ_2 solution. We checked the accuracy of our algorithm by using a slightly different ODE solver, and we estimate that our procedure determines Ψ to at worst a several percent error throughout the region of interest.

Typical contour plots of $\mathrm{Re}\Psi$ and $\mathrm{Im}\Psi$, for ϵ slightly below and slightly above ϵ_c, are presented in Figs. 4(a) and 4(b), respectively. Notice that there is only one zero in Ψ and this determines a unique eigenvalue ω^*. Of particular importance is the fact that $\mathrm{Re}\omega^*$ moves from above zero to below zero as ϵ goes from 0.14 to 0.16. This is in agreement with an estimate of $\epsilon_c\sim 0.15$ for this set of A and B parameters made in II. In Fig. 5 we plot $\mathrm{Re}\omega^*$ and $\mathrm{Im}\omega^*$ versus ϵ determined by iterating towards $\Psi=0$. These numbers agree quantitatively with the growth rate and frequency of the tip velocity in our numerical simulations reported in II. Thus the stability analysis around our preselected velocity accurately describes the oscillations around constant tip translation.

Several comments are in order. Consider a typical case of $\epsilon>\epsilon_c$. The actual small oscillation eigenvector is a

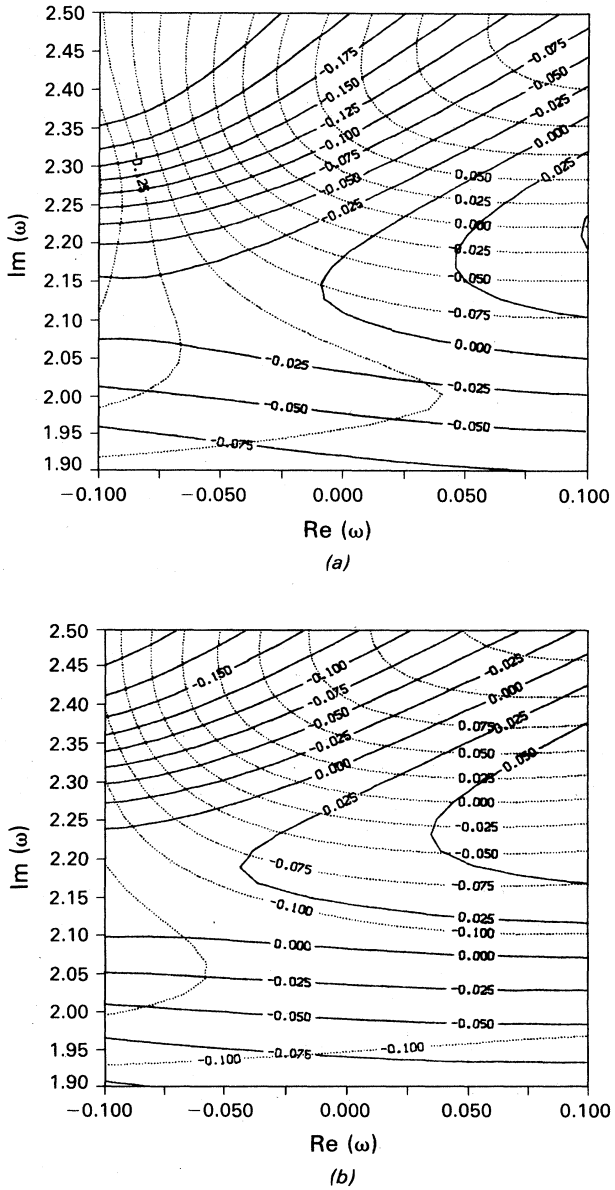

FIG. 4. Contour plot of $\Psi(\omega)$ for (a) $\epsilon=0.14$, (b) $\epsilon=0.16$. The solid lines are $\mathrm{Re}\Psi$ and the dotted lines are $\mathrm{Im}\Psi$.

particular linear superposition of the ϕ_1 and ϕ_2 solutions. It turns out for reasons that we do not fully understand that the wave vector q_2 always has a small positive real part (corresponding to exponential *growth),* whereas $\mathrm{Re}q_1$ is large and negative. Asymptotically ϕ_2 dominates, giving a sidebranch wave vector of $\mathrm{Im}q_2$. Since $\mathrm{Re}q_2\sim 0$, Eq. (5) predicts

$$V\,\mathrm{Im}q_2\sim-\mathrm{Im}\omega^*\ . \tag{7a}$$

This is exactly the requirement that side branches are almost stationary when viewed in the laboratory frame of reference. Furthermore, it seems to be always true that

$$V\,\mathrm{Re}q_2+\mathrm{Re}\omega^*>0 \tag{7b}$$

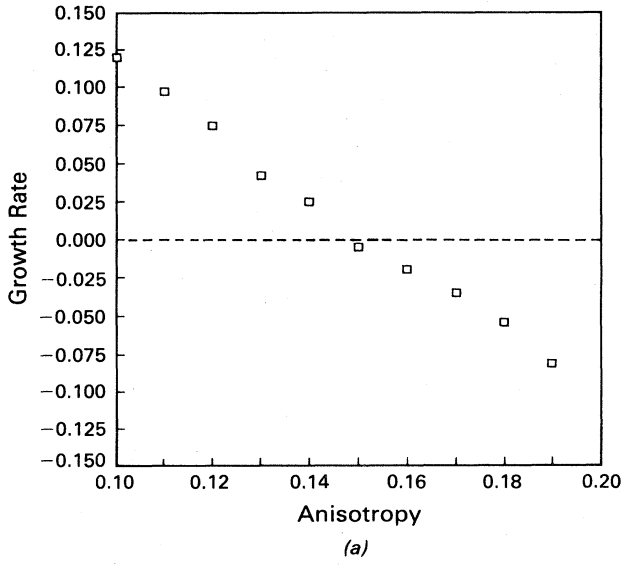

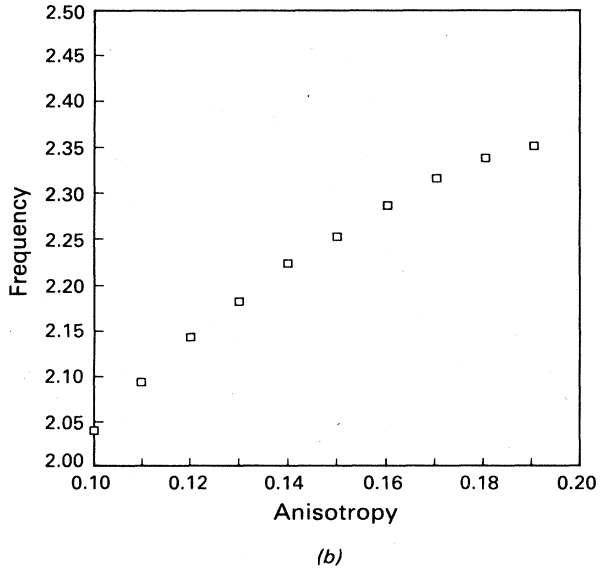

FIG. 5. Sidebranching eigenvalue as a function of ϵ; (a) real part (tip-perturbation growth rate) and (b) imaginary part (tip-oscillation frequency).

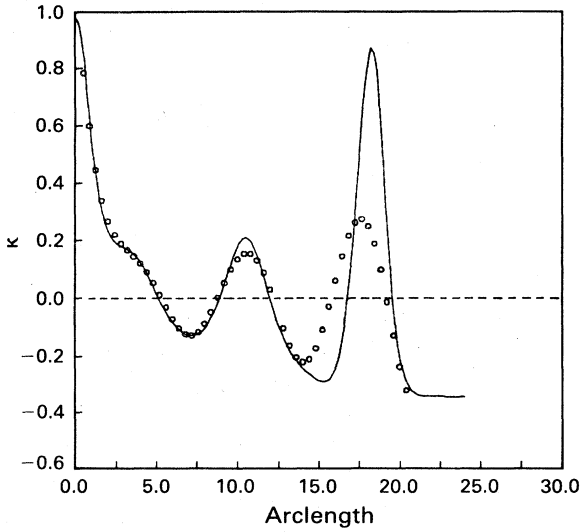

FIG. 6. Curvature plots: the solid line is the result of a direct numerical integration of (1), and the dots are the sum of the steady-state shape (2) and the leading linear perturbation mode.

even for stable ($\mathrm{Re}\omega^* < 0$) tip oscillations. This predicts that in the *laboratory frame* sidebranches continue to grow even as the tip velocity spirals down to a constant value (while in the reference frame of the moving tip they are left behind). Although the velocity is selected by convergence onto the steady-state solution, the asymptotic shape always contains an infinite train of side branches. This behavior does not quite correspond to that observed in dendritic crystals,[9] however, where sidebranching always exhibits neutral stability in the tip frame remaining a constant distance behind the tip.

In the cases we have investigated so far, all of the solutions with the exception of V^* have velocities which lie well below the stability point $\mathrm{Re}\omega^* = 0$. It is reasonable to speculate that this is always the case, that it is impossible for a secondary solution to be even approximately stable. If not, a system might in general be able to support several different modes of dendritic growth, the selection in a given case depending on the initial conditions.

We conclude this section with a comparison in Fig. 6 of a curvature plot generated by our numerical simulation program described in II, with a steady-state shape plus a linear perturbation approximated by its asymptotic form. We fix the complex amplitude of the perturbation by matching the first curvature minimum. Even with this rather crude approximation for the eigenvector, the system is clearly being described properly by our analysis. It is quite clear, for example, how the experimentally measurable sidebranch spacings are determined by the wave vector $\mathrm{Im}q_2$. At very large values of s, additional nonlinearities must be taken into account for a full description of the sidebranch dynamics.

IV. DISCUSSION

Let us summarize our findings. We have shown how the detailed phenomenology of dendritic growth in the local, geometrical evolution model can be understood as originating from a solvability condition selecting a discrete velocity and a discrete eigenmode around this velocity controlling the stability of the solution. In consequence, there is a critical anisotropy required to maintain stable dendritic growth. These findings represent a major success for the idea of using simplified models for growth processes. Because of the tractability of our equations, we have been able to propose a new approach to analyzing the dendritic growth patterns of our model.

We would now like to argue that a similar scenario should be valid for true diffusion-controlled evolution:[3] an interface coupled to a temperature field satisfying the diffusion equation and the Gibbs-Thompson boundary con-

dition $T_I = T_M(1 - d_0\kappa)$, where T_M is the melting temperature and d_0 is the capillary length. Our prediction is that the velocity is selected by the breakdown of the Ivantsov family of steady-state solutions, under the inclusion of surface tension, to a set of discrete solutions. The repeated sidebranching about a stable tip observed experimentally would be attributed to a new discrete eigenmode of the linear-stability operator. The stability of the tip with respect to splitting may require a critical anisotropy, depending on the magnitude of the dimensionless undercooling or Peclet number. (Note, however, that the detailed sidebranch behavior in the supercritical case does not entirely correspond to that found in our local model.) We know of no experimental data that could not, in principle, be explained by this type of approach.

In Ref. 10 we showed that the usual demonstrations that the Ivantsov solution could be extended to include nonzero surface tension were in fact inadequate to answer the question. The approach used there is reminiscent of the situation here: the equation near the tip cannot in general be integrated to have the proper approach to the zero-curvature fixed point. This fact is highly suggestive of the emergence of a solvability condition. A further indication of the universality of this behavior is afforded by the boundary-layer model of Ben-Jacob *et al.*[11] An analysis similar to the one performed in Sec. II can be used to show that there exists a discrete set of steady-state solutions,[12] although numerical simulations of this model have not advanced to the stage where they could be used to test our theory. Note that there is one aspect of dendritic growth that is reproduced more accurately by this type of boundary-layer model than by the local geometrical model studied here. The dendritic solution here approaches its asymptotic shape exponentially as opposed to the power-law behavior expected for the true Ivantsov problem and the boundary-layer model. The fact that this type of solvability constraint is also valid for the boundary-layer system,[11,12] as well as our earlier remarks regarding the breakdown of the Ivantsov solution, lead us to expect that this difference is not crucial for the selection mechanism.

Another pattern-selection problem with strong similarities to dendritic growth is Saffman-Taylor fingering.[13] In that problem, when one fluid displaces a more viscous one in a narrow gap between parallel plates or a porous medium, one finds in laboratory or numerical[14] experiments that the displacing fluid eventually forms a single finger which advances with constant velocity. Theoretically, there exists an infinite family of solutions which breaks down to a discrete set[5] when surface tension is included. Recent calculations[15] have shown that the velocity is determined by a solvability condition and again, the phenomenology is quite similar to what occurs in the geometrical model.

Finally, we would like to discuss some recent numerical simulations of the diffusion equation in the zero Peclet-number limit.[16] The early time evolution of the system has a finite-sized dendrite, and aside from a slow decrease in the tip velocity with time,[17] the system should behave as a standard crystal growth system. The fact that the system did not operate at a "marginally stable point," but instead underwent a transition from unstable to stable sidebranch emission as the amount of anisotropy varied, is further evidence for the validity of the mechanism we propose here.

ACKNOWLEDGMENTS

We would like to acknowledge useful discussions with R. F. Dashen, L. Kadanoff, and Y. Pomeau and would like to thank H. Aref and Y. Pomeau for sharing some of their results regarding Saffman-Taylor fingering prior to publication.

[1]R. C. Brower, D. Kessler, J. Koplik, and H. Levine, Phys. Rev. A **29**, 1335 (1984).
[2]D. Kessler, J. Koplik, and H. Levine, Phys. Rev. A **30**, 3161 (1984).
[3]For a review, see J. S. Langer, Rev. Mod. Phys. **52**, 1 (1980).
[4]J. S. Langer and H. Müller-Krumbhaar, Acta Metall. **26**, 1681 (1978); **26**, 1689 (1978); **26**, 1697 (1978).
[5]J. W. McLean and P. G. Saffman, J. Fluid Mech. **102**, 455 (1981); J.-M. Vanden-Broeck, Phys. Fluids **26**, 2033 (1983).
[6]D. G. Aronson and H. F. Weinberger, Adv. Math. **30**, 33 (1978); G. Dee and J. S. Langer, Phys. Rev. Lett. **50**, 383 (1983); J. S. Langer and H. Müller-Krumbhaar, Phys. Rev. A **27**, 499 (1983).
[7]G. P. Ivantsov, Dokl. Akad. Nauk SSR **58**, 567 (1947).
[8]L. M. Mack, J. Fluid Mech. **73**, 497 (1976).
[9]S. C. Huang and M. E. Glicksman, Acta Metall. **29**, 701 (1981); **29**, 717 (1981).
[10]R. C. Brower, D. Kessler, J. Koplik, and H. Levine, Scr. Metall. (to be published).
[11]E. Ben-Jacob, N. Goldenfeld, J. S. Langer, and G. Schön, Phys. Rev. Lett. **51**, 1930 (1983); Phys. Rev. A **29**, 330 (1984).
[12]D. Kessler and H. Levine (unpublished).
[13]P. G. Saffman and G. I. Taylor, Proc. R. Soc. London, Ser. A **245**, 312 (1958).
[14]H. Aref (private communication).
[15]Y. Pomeau (private communication).
[16]D. Kessler, J. Koplik, and H. Levine, Phys. Rev. A **30**, 2820 (1984).
[17]J. S. Langer (unpublished).